Phase field modeling of elasto-plastic deformation induced by diffusion controlled growth of a misfitting spherical precipitate

Kais Ammar[a]; Benoît Appolaire[b]; Georges Cailletaud[a]; Samuel Forest[a]

[a] Mines ParisTech, Centre des Matériaux, 91003 Evry cedex, France [b] LEM, CNRS, 92322 Châtillon, France

PLEASE SCROLL DOWN FOR ARTICLE

Taylor & Francis
Taylor & Francis Group

Phase field modeling of elasto-plastic deformation induced by diffusion controlled growth of a misfitting spherical precipitate

Kais Ammar[a], Benoît Appolaire[b]*, Georges Cailletaud[a] and Samuel Forest[a]

[a]*Mines ParisTech, Centre des Matériaux, CNRS UMR 7633, BP 87, 91003 Evry cedex, France;* [b]*LEM, CNRS, ONERA UMR 104, 29 Av. Division Leclerc, BP 72, 92322 Châtillon, France*

A phase field model accounting for plasticity has been developed using an homogenization scheme for interpolating the constitutive laws within the diffuse interface. The influence of plasticity on the growth of a misfitting spherical precipitate, controlled by solute diffusion has been investigated: plasticity in the matrix slows down the transformation. Moreover, an excellent agreement with the corresponding analytical sharp interface solutions has been achieved.

Keywords: phase field; diffusional transformation; elasto-plasticity; homogenization

In crystalline solids, diffusional phase transformations are often accompanied by deformations induced by changes in crystalline structures [1]. The stresses arising from the transformation strain can have a significant influence on equilibria (equilibrium compositions and volume fractions of the coexisting phases), as well as on the processes (nucleation, growth and coarsening) selecting the final morphology and spatial distribution. Modeling the interaction between mechanics and phase transformation not only gives fundamental insight into the formation of microstructures, but also provides the opportunity to engineer new microstructures with salient features for novel applications. The main difficulty of such a task is common to many free boundary problems: it lies in the tight coupling between the interface evolution and the fields. It becomes even more complicated when complex mechanical material behavior, ranging from heterogeneous elasticity to general elastoviscoplasticity, is involved.

The phase field method is particularly well-suited to address this issue. The introduction of elasticity in the phase field approach, initiated by Khachaturyan [1], has succeeded in predicting complex microstructure evolutions driven by the interplay of diffusion and elasticity [2,3]. It is only very recently that some phase field models have been enriched with nonlinear mechanical behavior, extending the range of applications and materials which can be handled by this approach (e.g. [4,5]).

---

*Corresponding author. Email: benoit.appolaire@onera.fr

In this work, the general formulation including plasticity into phase field, based on homogenization schemes, and recently proposed in [5], is used to study the effect of plastic accommodation on the diffusion-controlled growth of an elastic spherical misfitting precipitate into a infinite supersaturated elastoplastic matrix.

We start with the total Ginzburg–Landau free energy, expressed as the sum of four contributions, which is assumed to depend on the order parameter ϕ and its gradient, the concentration c, the elastic strain $\underset{\sim}{\varepsilon}^e$ and the set of internal variables A associated to material hardening:

$$F(\phi, \nabla\phi, c, \underset{\sim}{\varepsilon}^e, A) = \int_V \left[f_{\text{ch}} + f_e + f_p + \frac{\epsilon^2}{2} |\nabla\phi|^2 \right] dv, \tag{1}$$

where f_{ch}, f_e and f_p are, respectively, the chemical, elastic and plastic free energy densities, and where the gradient square of the phase field variable ϕ accounts for the interface energy. Considering a two-phase binary alloy, f_{ch} has two local minima corresponding to the two phases. It is obtained by a double well potential in ϕ added to a mixture of the bulk free energies of both phases f_α and f_β, convex w.r.t. ϕ [6]:

$$f_{\text{ch}}(\phi, c) = h(\phi) f_\alpha(c) + \overline{h}(\phi) f_\beta(c) + W g(\phi), \tag{2}$$

where $h(\phi) = \phi^2(3 - 2\phi)$, $\overline{h}(\phi) = 1 - h(\phi)$, $g(\phi) = \phi^2(1 - \phi)^2$, the subscripts α and β indicate the two coexisting phases and the densities f_α and f_β are chosen to be quadratic functions of the concentration only:

$$f_\alpha(c) = \frac{1}{2} k_\alpha (c - a_\alpha)^2 \quad \text{and} \quad f_\beta(c) = \frac{1}{2} k_\beta (c - a_\beta)^2. \tag{3}$$

k_α, k_β are the free energy curvatures w.r.t. concentration (assumed to be equal in the present study $k_\alpha = k_\beta = k$). a_α and a_β are the equilibrium concentrations for α and β phases, respectively [7].

The second term f_e in (1) accounts for energy contributions due to elastic effects. The effective elastic energy is expressed in terms of the elastic energies of both phases weighted by the complementary functions $h(\phi)$ and $\overline{h}(\phi)$. Taking a quadratic function of elastic strain tensor for $f_{e\alpha}, f_{e\beta}$, the elastic energy is defined on the basis of the properties and variables related to the different phases: the total strains $(\underset{\sim}{\varepsilon}_\alpha, \underset{\sim}{\varepsilon}_\beta)$, the eigenstrains $(\underset{\sim}{\varepsilon}_\alpha^\star, \underset{\sim}{\varepsilon}_\beta^\star)$, the plastic strain tensors $(\underset{\sim}{\varepsilon}_\alpha^p, \underset{\sim}{\varepsilon}_\beta^p)$ and the fourth-order tensor of elasticity moduli $(\underset{\approx}{\boldsymbol{C}}_\alpha, \underset{\approx}{\boldsymbol{C}}_\beta)$:

$$\begin{aligned} f_e &= h(\phi) f_{e\alpha} + \overline{h}(\phi) f_{e\beta} \\ &= \frac{1}{2} h(\phi) \, \underset{\sim}{\varepsilon}_\alpha^e : \underset{\approx}{\boldsymbol{C}}_\alpha : \underset{\sim}{\varepsilon}_\alpha^e + \frac{1}{2} \overline{h}(\phi) \, \underset{\sim}{\varepsilon}_\beta^e : \underset{\approx}{\boldsymbol{C}}_\beta : \underset{\sim}{\varepsilon}_\beta^e, \end{aligned} \tag{4}$$

where $\underset{\sim}{\varepsilon}_\psi^e = \underset{\sim}{\varepsilon}_\psi - \underset{\sim}{\varepsilon}_\psi^\star - \underset{\sim}{\varepsilon}_\psi^p$ (ψ stands for α or β).

Based on Voigt/Taylor model assumptions in homogenization theory, we assume that $\underset{\sim}{\varepsilon} = \underset{\sim}{\varepsilon}_\alpha = \underset{\sim}{\varepsilon}_\beta$ at each material point inside the diffuse interface region separating the elastoplastically inhomogeneous phases. The local effective stress is expressed in terms of the local stresses with respect to both phases. Taking Hooke's law into

account for each phase, the stress of heterogeneous materials is given as

$$
\begin{aligned}
\underset{\sim}{\sigma}(\underline{x}, t) &= h(\phi) \, \underset{\sim}{\sigma}_\alpha(\underline{x}, t) + \overline{h}(\phi) \, \underset{\sim}{\sigma}_\beta(\underline{x}, t) \\
&= h(\phi) \, \underset{\approx}{C}_\alpha : \underset{\sim}{\varepsilon}_\alpha^e + \overline{h}(\phi) \, \underset{\approx}{C}_\beta : \underset{\sim}{\varepsilon}_\beta^e.
\end{aligned} \tag{5}
$$

Then, it follows that the overall strain–stress relationship obeys Hooke's law:

$$
\underset{\sim}{\sigma} = \underset{\approx}{C}_{\text{eff}} : (\underset{\sim}{\varepsilon} - \underset{\sim}{\varepsilon}^p - \underset{\sim}{\varepsilon}^\star), \tag{6}
$$

where the local effective elasticity moduli C_{eff}, eigenstrain $\underset{\sim}{\varepsilon}^\star$ and plastic strain $\underset{\sim}{\varepsilon}^p$ vary continuously between their respective values in each phase:

$$
\underset{\approx}{C}_{\text{eff}} = h(\phi) \, \underset{\approx}{C}_\alpha + \overline{h}(\phi) \, \underset{\approx}{C}_\beta \tag{7}
$$

$$
\underset{\sim}{\varepsilon}^\star = \underset{\approx}{C}_{\text{eff}}^{-1} : (h(\phi) \, \underset{\approx}{C}_\alpha : \underset{\sim}{\varepsilon}_\alpha^\star + \overline{h}(\phi) \, \underset{\approx}{C}_\beta : \underset{\sim}{\varepsilon}_\beta^\star) \tag{8}
$$

$$
\underset{\sim}{\varepsilon}^p = \underset{\approx}{C}_{\text{eff}}^{-1} : (h(\phi) \, \underset{\approx}{C}_\alpha : \underset{\sim}{\varepsilon}_\alpha^p + \overline{h}(\phi) \, \underset{\approx}{C}_\beta : \underset{\sim}{\varepsilon}_\beta^p). \tag{9}
$$

Note that (8) and (9) differ from usual phase field schemes as discussed in [5]. Indeed, using homogenization schemes, the eigenstrain (8) and the plastic strain (9) are no longer the average of the local properties of both phases, contrary to the standard approach where properties follow some kind of mixture laws. The advantage of our approach makes possible to mix different types of constitutive equations for each phase, e.g. hyperelastic nonlinear behavior for one phase and conventional elastic–plastic model with internal variables for the other one.

A third contribution f_p due to hardening effects in each phase can be added to the free energy density. In this work, hardening is not considered, and isotropic von Mises rate independent plasticity without hardening is used for the β phase [8]. The corresponding yield function is

$$
g(\underset{\sim}{\sigma}_\beta) = J_2(\underset{\sim}{\sigma}_\beta) - \sigma_\beta^0 \quad \text{and} \quad J_2(\underset{\sim}{\sigma}_\beta) = \sqrt{\frac{3}{2} \, \underset{\sim}{s}_\beta : \underset{\sim}{s}_\beta}, \tag{10}
$$

where $J_2(\underset{\sim}{\sigma}_\beta)$ is the von Mises equivalent stress, $\underset{\sim}{s}_\beta$ is the deviatoric stress and σ_β^0 is the yield stress in the β phase.

The main differences among the phase-field models lie in the treatment of the various contributions to the total free energy. Once the total free energy is defined, the governing equations of the fields are described by the time-dependent kinetic equations, which are the Ginzburg–Landau equation for the non-conserved order parameter $\phi(x, t)$, the mass balance for the conserved concentration field $c(x, t)$ and the static equilibrium for the stress tensor $\underset{\sim}{\sigma}(x, t)$ in the absence of volume forces:

$$
\begin{aligned}
-\frac{1}{M}\dot{\phi} + \epsilon^2 \Delta\phi - \frac{\partial f_{\text{ch}}}{\partial \phi} - \frac{\partial f_e}{\partial \phi} - \frac{\partial f_p}{\partial \phi} &= 0 \\
\dot{c} + \nabla.\left[-L(\phi)\left(\nabla \frac{\partial f_{\text{ch}}}{\partial c} + \nabla \frac{\partial f_e}{\partial c} + \nabla \frac{\partial f_p}{\partial c} \right) \right] &= 0 \\
\nabla.\underset{\sim}{\sigma} &= 0,
\end{aligned} \tag{11}
$$

Table 1. Data used in the calculations.

E/k	ν	$\varepsilon^\star$	σ_β^0/k	$\gamma/(kR)$	δ/R	$D\tau/R^2$	a_α	a_β
7×10^{10}	0.3	3×10^{-4}	12.5	5×10^{-3}	10^{-3}	0.1	0.7	0.3

where M is the phase field mobility and $L(\phi)$ the Onsager coefficient, defined with respect to the chemical diffusivities D_α and D_β in both phases by means of the complementary functions $h(\phi)$ and $\overline{h}(\phi)$ [7]:

$$L(\phi) = h(\phi)D_\alpha/k_\alpha + \overline{h}(\phi)\, D_\beta/k_\beta. \tag{12}$$

In order to illustrate some non-trivial effects of plasticity on the kinetics of diffusional phase transformation, we have investigated the growth of an elastic spherical precipitate of radius r_{int} into a spherical supersaturated elastoplastic matrix of radius R. Indeed, exact analytical solutions (recalled here for self-consistency) for the strain/stress fields are given in [9] for infinite matrix $R \to \infty$. Assume that the eigenstrains are spherical tensors independent of concentration, and choose β as the stress free reference state $\underset{\sim}{\varepsilon_\beta^\star} = \underset{\sim}{\mathbf{0}}$ and $\underset{\sim}{\varepsilon_\alpha^\star} = \varepsilon^\star \underset{\sim}{\mathbf{I}}$, where $\underset{\sim}{\mathbf{I}}$ is the identity second order tensor. If both phases are considered to behave in a purely elastic state, the analytical solution for isotropic elasticity is given in spherical coordinates as

$$\begin{cases} \sigma_{rr} = \sigma_{jj} = -p_e & r \leq r_{\text{int}} \\ \sigma_{rr} = -2\sigma_{jj} = -p_e \left(\dfrac{r_{\text{int}}}{r}\right)^3 & r \geq r_{\text{int}} \end{cases}, \tag{13}$$

where jj stands for $\theta\theta$ and $\varphi\varphi$, and $p_e = 2E/[3(1-\nu)]\varepsilon^\star$. If the matrix behavior is isotropic elasto-plastic, the analytical solutions for the strain/stress fields involve the size of the plastic zone, as given in [9]:

$$\begin{cases} \sigma_{rr} = \sigma_{jj} = -p & r \leq r_{\text{int}} \\ \sigma_{rr} = \sigma_{jj} - \sigma_\beta^0 = -p + 2\sigma_\beta^0 \log\left(\dfrac{r}{r_{\text{int}}}\right) & r_{\text{int}} \leq r \leq r_p \\ \sigma_{rr} = -2\sigma_{jj} = -2/3\, \sigma_\beta^0 \left(\dfrac{r_p}{r}\right)^3 & r \geq r_p, \end{cases} \tag{14}$$

where $r_p = r_{\text{int}}\left[3p_e/(2\sigma_\beta^0)\right]^{1/3}$ is the interface between the elastic zone and the elastoplastic zone inside the matrix, and $p = -[2\sigma_\beta^0 \log(r_p/r_{\text{int}}) + 2\sigma_\beta^0/3]$. These analytical results, classical in the mechanical context and based on a perfect sharp interface without surface energy, can be compared to the results of the proposed phase field model where the interface is diffuse. The data used in the calculations are summarized in Table 1: the Young's modulus E, Poisson ratio ν and chemical diffusivity D are assumed to be the same in both phases. The interfacial energy and thickness are denoted, respectively, by γ and δ. All parameters are dimensionless and scaled with the chemical free energies curvature k, a mesoscopic length (typically size R) and the characteristic time $\tau = \beta/k$ related to interface motion.
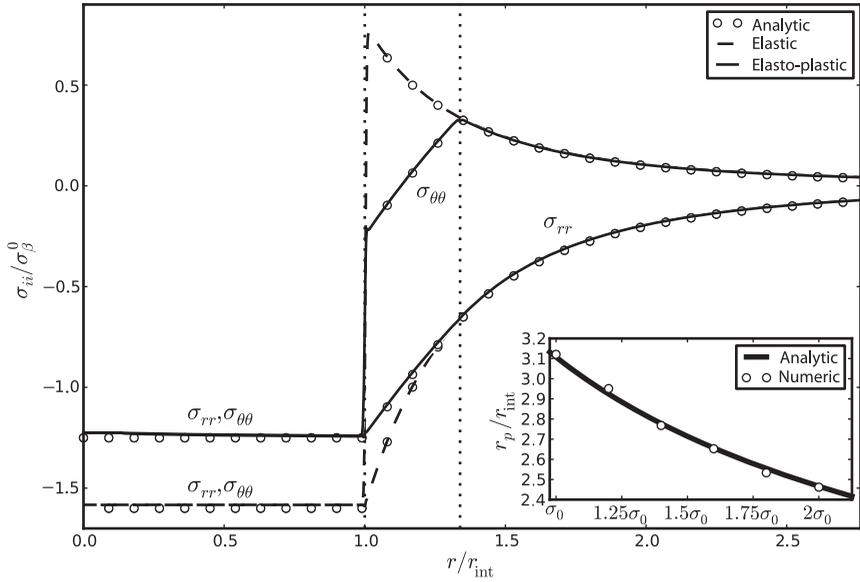
Figure 1. Profiles of normal σ_{rr} and tangential $\sigma_{\theta\theta}$ stress components for matrices with purely elastic and ideal plastic behaviors, compared for the same value of r_{int}. Relative interface thickness is $\delta/r_{\text{int}} = 0.014$.

The finite element method has been used to solve the problem, with a mesh composed of quadratic eight-nodes quadrangular elements. The following free surface boundary conditions have been applied at $r = R$:

$$\nabla\phi \cdot \underline{n} = 0, \quad \nabla c \cdot \underline{n} = 0 \quad \text{and} \quad \sigma_{rr} = 0. \tag{15}$$

Initially, we have imposed $\phi = [1 - \tanh(2r'/\delta)]/2$ and $c = a_\alpha + (a_\beta - a_\alpha)[1 - \tanh(2r'/\delta)]/2$, with $r' = r - r_0$, corresponding to an inner spherical α precipitate with radius r_0 embedded into the β matrix shell with outer radius $R \gg r_0$. Moreover, we have set $\delta/r_0 = 0.1$ so as to avoid spurious effects associated with large interface thickness.

First, we compare in Figure 1 the profiles of the stress components σ_{rr} and $\sigma_{\theta\theta}$ generated by the misfitting precipitate, at a given time, when the matrix is either purely elastic (dashed lines), or ideal plastic (continuous lines). The components are normalized by the yield stress σ_β^0, and the space coordinate r by the precipitate radius r_{int}. The precipitate/matrix interface is localized by the first vertical dotted line at $r/r_{\text{int}} = 1$ and the plastic zone radius by the second one. Calculations with the phase field are plotted with lines, and compared with the analytical solutions with symbols. The well-known result [10] that the stress within the precipitate is uniform and hydrostatic is recovered.

Differences between the elastic and ideal plastic cases are significant only within the precipitate and in the plastic zone. The hydrostatic stress in the inclusion is indeed smaller in the plastic case, as expected. Inside the plastic zone, the tangential stress $\sigma_{\theta\theta}$ with plasticity differs fundamentally from its elastic counterpart: the latter
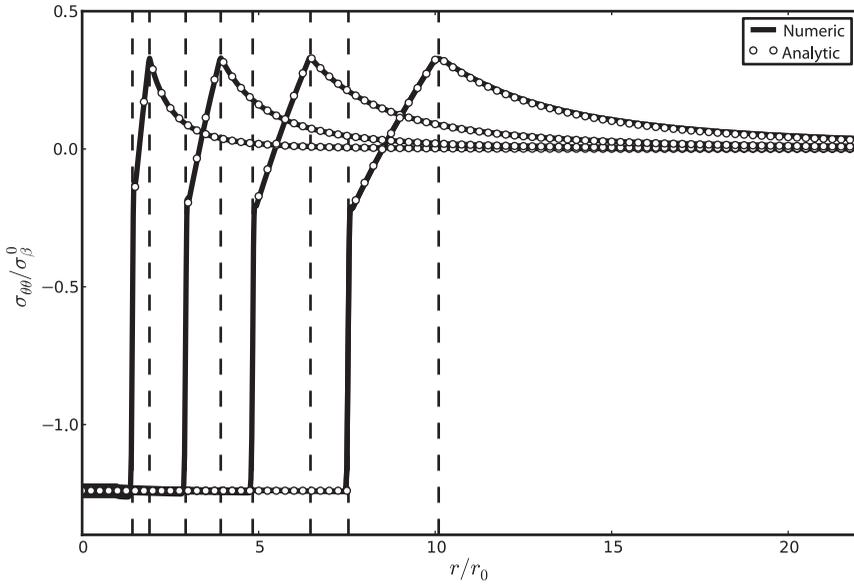
Figure 2. Profiles of $\sigma_{\theta\theta}$ versus time: phase field (continuous lines) and analytical solution (Equation (14)) (open symbols). Interface and plastic radius are located by vertical dashed lines.

decreases with r from a maximum positive value at the interface whereas the former increases from a negative value at the interface to a positive maximum value at r_p. Hence, The slope of $\sigma_{\theta\theta}$ experiences a discontinuity at r_p due to the discontinuity in the slope of the stress–strain curve at the yield point. A very good agreement is achieved between our calculations and the analytical solutions for a sufficiently thin interface.

The evolution of $\sigma_{\theta\theta}$ during growth is plotted in Figure 2, in the plastic case. The stress remains hydrostatic and constant within the precipitate as long as the free external boundaries do not interact with the stress field, similarly to what is predicted by the Eshelby inclusion model in the pure elastic case. Moreover, the values of $\sigma_{\theta\theta}$ bounding the plastic zone exhibit only slight changes during growth whereas the plastic zone extends quite significantly. As shown in Figure 2, our calculations agree very well with the analytical solution all along the growth.

The influence of plasticity on the growth kinetics is shown in Figure 3, where the precipitate radius (normalized by the initial one r_0) is plotted versus time for three cases: chemical, elastic and ideal plastic. Concentration profiles for the three cases are plotted in the inset for the same time, showing that the growth is controlled by diffusion in the matrix.

After transients, short with respect to the total time ($<10^4$ s), the growth laws are all parabolic, i.e. $r_{int} = K\sqrt{t}$. The chemical case (black) is the fastest, when the plastic one is the slowest, quite unexpectedly. In order to understand these trends, we have compared our results with the analytical solutions of the sharp interface model proposed by Zener [11]. This model relies on solving Fick's equation in an infinite
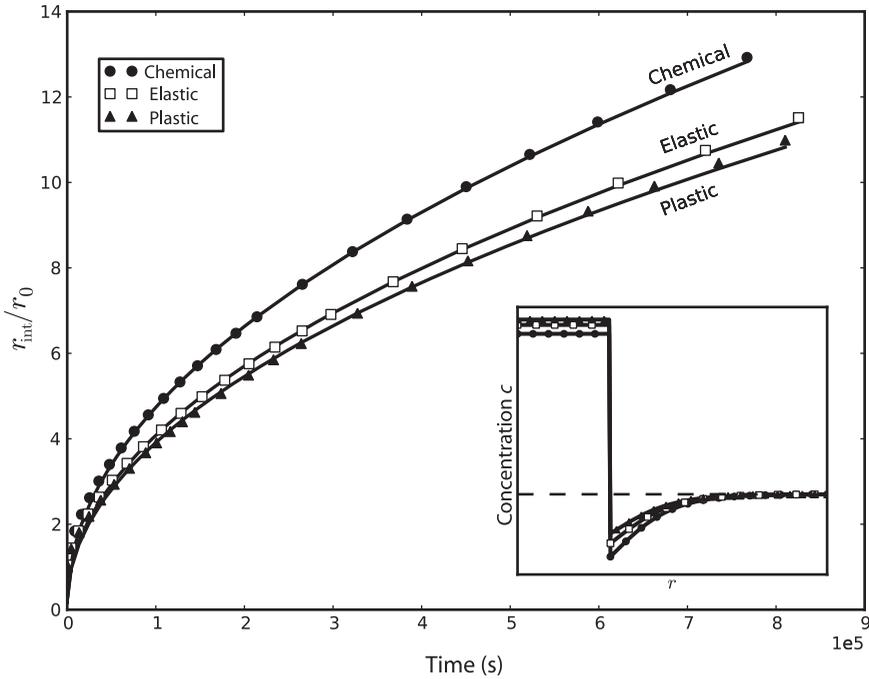
Figure 3. Growth kinetics of a misfitting spherical precipitate: chemical (dots), elastic (squares) and ideal plastic (triangles). Phase field with symbols and analytical solution with lines.

supersaturated matrix surrounding a growing stoichiometric spherical precipitate. Assuming that the concentrations at the interface remain constant (e.g. given by the phase diagram at constant temperature), the solute balance gives the growth constant K as the solution of the following relation:

$$2\,\text{Pe}\,\exp(\text{Pe})\Big[\exp(-\text{Pe}) - \sqrt{\pi\text{Pe}}\,\text{erfc}(\sqrt{\text{Pe}})\Big] = \Omega, \tag{16}$$

where $\Omega = (c_\beta - c_\beta^0)/(c_\beta - c_\alpha)$ is the matrix supersaturation depending on the interfacial concentrations c_α, c_β and the matrix concentration c_β^0 far away from the interface; $\text{Pe} = K^2/(4D)$ is the Péclet number involving the solute diffusivity D. The interfacial concentrations c_α and c_β depend on local stresses and strains according to the thermodynamics of stressed crystalline solids (e.g. [12]). Assuming that equal free energy curvatures $k_\alpha = k_\beta = k$, we obtain

$$c_{\alpha,\beta} = a_{\alpha,\beta} + (\mathcal{E} + \kappa\gamma)/(k\,\Delta a), \tag{17}$$

$$\mathcal{E} = \Delta f_\text{e} - \mathcal{E}_\text{coh} = \Delta f_\text{e} - \underset{\sim}{\sigma}_\beta : \Delta\underset{\sim}{\varepsilon}, \tag{18}$$

where $\Delta\psi = \psi_\alpha - \psi_\beta$ denotes the jump of any value ψ (a, f_e or $\underset{\sim}{\varepsilon}$) across the interface, κ is the interface mean curvature and γ its energy. The term $\mathcal{E}$ accounting for mechanics is composed of two contributions: the jump Δf_e of elastic energy density

across the interface, and $\mathcal{E}_{\mathrm{coh}}$ which represents the elastic energy necessary to keep both lattices coherent across the interface [12]. It must be emphasized that $\mathcal{E}_{\mathrm{coh}}$ involves the jump of total deformations. Using the solution equations (13) and (14), we have $\mathcal{E} = \mathcal{E}_{\mathrm{e}} = E_\alpha (\varepsilon^\star)^2 / (1 - \nu_\alpha)$ in the purely elastic case. In the ideal plastic case, our analytical computations give $\mathcal{E}_{\mathrm{p}} = 1.37 \; \mathcal{E}_{\mathrm{e}}$ for the parameters of Table 1. According to the above equations, a dilatational misfit in the precipitate raises the interfacial concentrations in both phases due to the positive jump $\mathcal{E}$: consequently, the concentration gradient in the matrix decreases at the interface, as illustrated in the inset of Figure 3, and so does the supersaturation Ω in Equation (16). This leads to smaller K and slower growth kinetics as compared to the chemical case. Moreover, the plastic relaxation around the precipitate induces jumps of total strains larger than in the elastic case due to $\underset{\sim}{\varepsilon}_\beta^p$: $|\mathcal{E}_{\mathrm{coh}}|$ increases and $\mathcal{E}_{\mathrm{p}} > \mathcal{E}_{\mathrm{e}}$. Consequently, the concentration profile in the β matrix flattens with plasticity, and the growth slows down. It is worth noting that our calculations are in excellent agreement with the analytical solutions, as shown in Figure 3. This puts our model on a firmer footing for investigating more complex configurations and morphologies.

In the present study, misfits, elastic constants and yield stresses have been assumed not to depend on the concentration. Therefore, there is no contribution of elasticity and plasticity in the diffusion equation $(11)_b$, because $\partial f_e / \partial c = \partial f_p / \partial c = 0$. Unfortunately, it is not trivial to qualitatively assess what role would those terms play because they can contribute both in the bulk and at the interface. Further calculations are thus necessary for clarifying their influence on growth.

Finally, it is worth mentioning that very thin interfaces have been considered in this work for accurately recovering the stress fields predicted by the sharp interface solutions. This would be very penalizing from a computational point of view for dealing with 2D or 3D microstructures. Hence, it seems necessary to investigate the influence of the ratio $\delta / r_{\mathrm{int}}$ on the results in future work.

In summary, we have developed a phase field model accounting for plasticity using an homogenization scheme for interpolating the constitutive laws within the diffuse interface. This framework allows combining very different constitutive laws with great flexibility. We have investigated the influence of plasticity on the growth of a misfitting spherical precipitate, controlled by solute diffusion. Quite unexpectedly, the growth rate decreases when the stresses in the matrix are relaxed by plasticity. Note that this behavior differs for the case of plane interfaces [13]. This trend has been analyzed and confirmed by comparing our results with analytical solutions of the corresponding problem.

References

[1] A.G. Khachaturyan, *Theory of Structural Transformations in Solids*, John Wiley & Sons, New York, 1983.
[2] Y. Le Bouar and A.G. Khachaturyan, Acta Mat. 48 (2000) p.1705.
[3] G. Boussinot, A. Finel and Y. Le Bouar, Acta Mat. 57 (2009) p.921.
[4] A. Gaubert, Y. Le Bouar and A. Finel, Phil. Mag. 90 (2010) p.375.
[5] K. Ammar, B. Appolaire, G. Cailletaud and S. Forest, Eur. J. Comp. Mech. 18 (2009) p.485.

[6] N. Moelans, B. Blanpain and P. Wollants, Comp. Coupl. Ph. Diag. Thermochem. 32 (2008) p.268.
[7] K. Ammar, B. Appolaire, G. Cailletaud, F. Feyel and S. Forest, Comp. Mat. Sci. 45 (2009) p.800.
[8] J. Besson, G. Cailletaud, J.-L. Chaboche, S. Forest and M. Blétry, *Non-linear Mechanics of Materials*, Springer, Berlin, 2010.
[9] J.K. Lee, Y.Y. Earmme, H.I. Aaronson and K.C. Russell, Metal. Trans. A 11 (1980) p.1837.
[10] J.D. Eshelby, Proc. Roy. Soc. Lond. A 241 (1957) p.376.
[11] C. Zener, J. Appl. Phys. 20 (1949) p.950.
[12] W.C. Johnson and J.I.D. Alexander, J. App. Phys. 9 (1986) p.2735.
[13] K. Ammar, *Modeling and simulation of phase transformation-mechanics coupling using a phase field method*. PhD Thesis, Mines ParisTech, 2010.